REGULARIZED FORMULATION FOR OPTIMAL DESIGN OF AXISYMMETRIC PLATES

KENG-TUNG CHENG† and NIELS OLHOFF

Department of Solid Mechanics, The Technical University of Denmark, Lyngby, Denmark

Abstract—This paper presents a regularized mathematical formulation, necessary conditions of optimality and solutions of problems of optimal design of solid, elastic, axisymmetric plates of prescribed total material volume. Single-purpose design criteria of minimum static compliance (maximum stiffness) and maximum frequency of free, transverse vibrations, are considered.

The regularization, which alleviates some anomalies and difficulties encountered earlier in plate optimization problems, is based on a new compound plate model with two simultaneous design variables, namely, variable thickness of a solid part of the plate and variable concentration of a dense system of thin, integral stiffeners attached to the solid plate part. A numerical, optimality-criterion-based method of solution is developed for the problem, and several optimal designs are presented. The results are compared with results obtained from optimal design formulations applied heretofore, and substantiate the superiority of the new, regularized formulation.

1. INTRODUCTION

Problems of determining optimal thickness distributions for thin, solid elastic plates have attracted considerable interest in the last decade. It is now accepted[1–4] that optimal solutions do not exist to geometrically unconstrained problems, i.e. problems where no constraints are specified for the plate thickness function, but that such problems may possess several local optimal solutions. Quite naturally, it was speculated that specification of both maximum and minimum constraint values for the plate thickness function would ensure a global optimal solution[5], and several papers dealing with geometrically constrained plate optimization problems have indeed been published, see e.g. [6–8]. However, numerical difficulties are also reported[7, 8].

As a matter of fact, it has recently been shown by the authors[9] that even if minimum and maximum thickness constraints are considered, the traditional optimal design formulation, where the plate thickness function is used as the only design variable, is, in general, inadequate. The reason for this is that the aforementioned choice of design variable confines the design space to the class of continuous functions or piecewise continuous functions with a finite number of discontinuities, and the global optimal design does not generally belong to this class of functions. Thus, the results of [9] clearly indicate that the global optimal design for a given problem will, in general, be a plate which, at least in some sub-regions, is equipped with an infinite number of infinitely thin stiffeners.

In order to be able to determine a possible global optimal plate design of this type, it is therefore necessary to regularize the mathematical formulation of the geometrically constrained optimization problem. In Refs. [10, 11], dealing with optimization of axisymmetric plates for minimum compliance and maximum frequency of transverse vibrations, respectively, the problems are regularized on the basis of a new plate model, which consists of a solid plate part equipped with a dense system of infinitely thin integral stiffeners of variable concentration. However, to gain simplicity in the numerical solution procedures in Refs. [10, 11], the thickness of the solid plate part is, in both papers, made equal to the minimum constraint value, i.e. the concentration of integral stiffeners is treated as the only design variable in the numerical examples. In spite of this restriction, the corresponding, simplified, integrally stiffened plate model is superior to the traditional, solid plate model for a vast majority of problems, although there are some exceptions[10]. In fact, the possible global optimal design of a thin elastic plate must be expected to be a compound plate, which contains both integrally stiffened sub-regions

---

†Visiting from the Department of Solid Mechanics, The Dalien Engineering Institute, Dalien, The People's Republic of China.

and purely solid sub-regions of variable thickness. However, the aforementioned restriction introduced in Refs. [10, 11] has prevented us from obtaining optimal plate designs of this compound type.

The present paper is a follow-up of Refs. [10, 11], with the objective of determining possible global optimal plate designs of the compound type. In Section 2 we formulate the minimum compliance design problem for axisymmetric plates on the basis of the generalized, new plate model, that is, we apply both the thickness of the solid plate part and the concentration of attached integral stiffeners as design variables. The necessary conditions of optimality are derived in Section 3, and we develop some theoretical results concerning the behaviour of the optimal design in the neighbourhood of plate edges of different boundary conditions. The problem of optimizing an axisymmetric plate for maximum frequency of free, transverse vibrations is taken up in Section 4, and it is shown that the previous developments of the paper can, either directly or in a very simple manner, be extended to this problem. Finally, in Section 5 we present several solutions to the regularized formulations of the two kinds of optimization problems considered, and comparing them to solutions obtained to earlier formulations in the literature, ascertain the superiority of the regularized formulation. A numerical solution procedure based on successive iterations is given in an appendix.

2. A MATHEMATICAL REFORMULATION OF THE OPTIMAL DESIGN PROBLEM FOR AXISYMMETRIC PLATES

We consider the problem of finding the theoretically best plate model and mathematical formulation for optimal design of axisymmetric, thin, elastic, solid plates, whose thickness h is variable and identifies the distance between the upper and lower plate surface, which are assumed to be disposed symmetrically with respect to the plate mid-plane. The total plate volume is assumed to be specified, and in addition, maximum and minimum constraint values h_{max} and h_{min} for the plate thickness function, pertinent material properties, the inner and outer radii of the plate (which may be annular), and the boundary conditions, are assumed to be given.

For exemplification, in the present and the following main section, we consider minimum compliance, i.e. maximum integral stiffness, as the design objective. We adopt a polar coordinate system with origin in the plate centre, and assume for the minimum compliance problem that the distribution of static load $p(r, \theta)$ is of the special type

$$p(r, \theta) = f(r) \cos n\, \theta, \tag{1}$$

where $f(r)$ is a given, θ-independent function, and n, a given integer. If homogeneous boundary conditions are specified for the axisymmetric plate, the plate deflection function $W(r, \theta)$ then attains the simple form

$$W(r, \theta) = w(r) \cos n\, \theta, \tag{2}$$

where $w(r)$ is independent of θ.

2.1 Traditional formulation

In the traditional formulation for optimal design, the plate thickness $h(r)$ is used as the design variable, and the optimal solution is assumed to be a solid plate. In dimensionless form, where the inner and outer radii for an annular plate are R_i and 1, respectively, and we have $R_i = 0$ for a full plate, the problem is posed as follows

With $h(r)$ as the design variable, minimize

$$\pi = \int_\Omega f(r) w(r) r\, dr \tag{3}$$

subject to the constraints

$$\int_\Omega h(r)r\,dr = 1,$$

$$h_{min} \le h(r) \le h_{max},$$

where

$$r \in \Omega\{r|R_i \le r \le 1\}.$$

Within this formulation, the optimal thickness distribution $h(r)$ is sought in the class of continuous functions or piecewise continuous functions with a finite number of discontinuities, and the plate bending rigidity D is assumed to be isotropic, i.e. independent of orientation, and given by $D = Eh(r)^3/12(1 - v^2)$, where E is Young's modulus and v is Poisson's ratio of the plate material. The optimization problem has been considered in this form in several papers, see e.g. Refs. [6–8]. However, as has recently been shown by the authors [9], the optimal thickness distribution will generally not belong to the aforementioned class of functions. As a matter of fact, if the given constraint values h_{max} and h_{min} differ sufficiently from each other, the optimal thickness function will exhibit an infinite number of discontinuities in certain sub-regions of the plate domain Ω. Optimal thickness functions of this type can obviously not be determined on the basis of the traditional formulation, and it is therefore necessary to reformulate the optimization problem.

2.2 New, regularized formulation with two design variables

In order to be able to determine a possible global optimal design subject to any given set of values of h_{max} and h_{min} for an axisymmetric plate, we now expand our design space by constructing a new, generalized plate model. This model covers an axisymmetric, integrally stiffened plate consisting of a solid part of variable thickness $h_s(r)$, $0 < h_{min} \le h_s \le h_{max}$ that is equipped with a system of infinitely thin integral stiffeners of variable concentration $\mu(r)$. Figure 1 shows a radial section through a small ring element of the plate. The element has the radial extent Δr and is equipped with a finite number of stiffeners. Each stiffener is circumferential, has rectangular cross-section of height $h_{max} - h_s$, and is placed symmetrically with respect to the plate mid-plane. The concentration $\mu(r)$ (or density) of the integral stiffeners is defined by

$$\mu(r) = \lim_{\Delta r \to 0} \frac{\sum_i \Delta c_i}{\Delta r}, \quad 0 \le \mu(r) \le 1, \tag{4}$$

where Δc_i is the width of the i'th stiffener of the element.
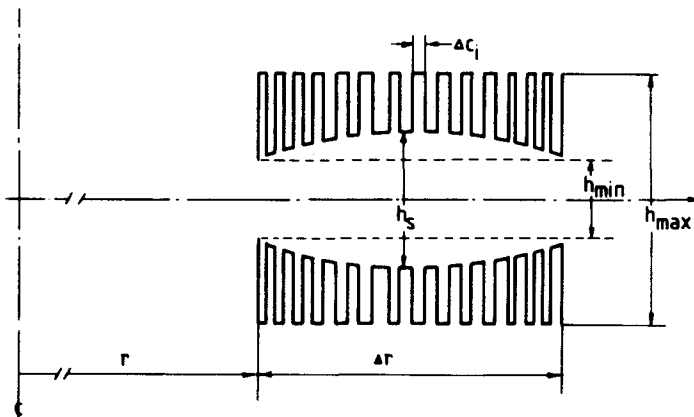

Fig. 1. Radial section through axisymmetric, integrally stiffened plate element of small radial extent Δr.

Note that this plate model, for $\mu(r) \equiv 0$ and $h_s \equiv h$, reduces to the solid plate of variable thickness $h(r)$ used in the traditional formulation for optimal design. On the other hand, for $\mu(r) \neq 0$ and $h_s \equiv h_{min}$, the model comprises another special case, namely the integrally stiffened plate model with $\mu(r)$ as the only design variable, which has very recently been used in Refs. [10, 11] for determining a number of numerical results that are superior to results obtained by means of the traditional formulation.

While integrally stiffened plate regions are excluded by the former special case plate model ($\mu \equiv 0$, $h_s \equiv h$), and solid regions of intermediate thickness are excluded by the latter ($\mu \neq 0$, $h_s \equiv h_{min}$), it is our objective in the following to demonstrate by means of a number of numerical results that the new generalized plate model is superior to those applied previously. In fact, it turns out that the optimal plate will, in general, be a compound plate that contains both sub-regions with integral stiffeners and sub-regions that are purely solid and of inter-mediate thickness.

By means of the new plate model with its two design variables $\mu(r)$ and $h_s(r)$, we now reformulate the plate optimization problem as follows:

With $h_s(r)$ and $\mu(r)$ as design variables, minimize

$$\pi = \int_\Omega f(r)w(r)r\,dr$$

subject to the constraints

$$\int_\Omega [h_s(r) + \mu(r)(h_{max} - h_s(r))]r\,dr = 1,$$

$$h_{min} \le h_s(r) \le h_{max}, \tag{5}$$

$$0 \le \mu(r) \le 1,$$

where

$$r \in \Omega\{r | R_i \le r \le 1\}.$$

Now, since the optimal plate is geometrically anisotropic (cylindrically orthotropic) in possible sub-regions with $0 < \mu(r) < 1$, it is necessary to consider the plate bending rigidity as a tensor (i.e. to depend on orientation) in the moment-curvature relationships (Hooke's law) for such sub-regions of the plate. In Refs. [10, 11] the components of the bending rigidity tensor are determined via two different paths, and we therefore just cite the results in what follows.

On the basis of Kirchhoff plate theory and with deflections in the form of eqn (2), the θ-independent factorials κ_{rr}, $\kappa_{\theta\theta}$ and $\kappa_{r\theta}$ of the radial, circumferential and twisting curvatures are given by

$$\kappa_{rr} = w'', \quad \kappa_{\theta\theta} = \frac{w'}{r} - \frac{n^2 w}{r^2}, \quad \kappa_{r\theta} = -\left(\frac{nw}{r}\right)', \tag{6}$$

respectively, where primes denote differentiation with respect to r. The moment-curvature relations read[10]

$$m_{rr} = D_r(\kappa_{rr} + \nu\kappa_{\theta\theta}), \quad m_{\theta\theta} = D_\theta(\kappa_{\theta\theta} + \nu_r\kappa_{rr}), \quad m_{r\theta} = D_{r\theta}(1 - \nu)\kappa_{r\theta} \tag{7a}$$

or in inverse form,

$$\kappa_{rr} = \frac{\nu(m_{rr} - \nu_r m_{\theta\theta})}{\nu_r D_{r\theta}(1 - \nu^2)}, \quad \kappa_{\theta\theta} = \frac{m_{\theta\theta} - \nu m_{rr}}{D_{r\theta}(1 - \nu^2)}, \quad \kappa_{r\theta} = \frac{m_{r\theta}}{D_{r\theta}(1 - \nu)}, \tag{7b}$$

where m_{rr}, $m_{\theta\theta}$ and $m_{r\theta}$ are the θ-independent factorials of the radial and circumferential bending moments and the twisting moment, respectively. In eqns (7a, b), ν is Poisson's ratio of

the isotropic, linearly elastic plate material, and the components D_r, $D_{r\theta}$ and D_θ of the plate bending rigidity tensor, together with the symbol ν_r, are given by[10, 11]

$$D_r = \frac{D_{max}D_s}{\mu D_s + (1-\mu)D_{max}}, \quad D_{r\theta} = \mu D_{max} + (1-\mu)D_s, \quad D_\theta = (1-\nu^2)D_{r\theta} + \nu^2 D_r, \quad \nu_r = \nu \frac{D_r}{D_\theta}, \quad (8)$$

respectively, where D_{max} and D_s are suitably non-dimensionalized scalar bending rigidities defined by

$$D_{max} = h_{max}^3, \quad D_s = h_s^3. \tag{9}$$

Equations (7a, b) express by means of eqns (8) and (9) the moment-curvature relationships in possible cylindrically orthotropic sub-regions of the plate where $0 < \mu(r) < 1$ and $h_s < h_{max}$. However, the above equations reduce precisely to the corresponding well-known relationships for isotropic plates in those sub-regions in which the plate is purely solid, that is, where $\mu = 0$ (purely solid sub-region with plate thickness h_s, $h_{min} \le h_s \le h_{max}$), or where $\mu = 1$ (purely solid sub-region with plate thickness h_{max}). Consequently, we can apply eqns (7a, b)–(9) throughout the plate in the following.

3. NECESSARY CONDITIONS FOR OPTIMALITY

The governing optimality equations for the regularized minimum compliance design problem (5) can be derived by variational analysis. The compliance π in (5) can alternatively be written as [10]

$$\pi = \int_\Omega \{D_{r\theta}[(1-\nu^2)\kappa_{\theta\theta}^2 + 2(1-\nu)\kappa_{r\theta}^2] + D_r(\kappa_{rr} + \nu\kappa_{\theta\theta})^2\} r \, dr, \tag{10}$$

and we may use this expression in constructing an augmented functional π^* defined by

$$\pi^* = \int_\Omega \{D_{r\theta}[(1-\nu^2)\kappa_{\theta\theta}^2 + 2(1-\nu)\kappa_{r\theta}^2] + D_r(\kappa_{rr} + \nu\kappa_{\theta\theta})^2\} r \, dr$$

$$- \Lambda\left\{\int_\Omega [h_s + \mu(h_{max} - h_s)] r \, dr - 1\right\}$$

$$- \int_\Omega \lambda[h_s - h_{max} + \sigma^2] r \, dr - \int_\Omega \beta[h_{min} - h_s + \tau^2] r \, dr \tag{11}$$

$$- \int_\Omega \gamma[\mu - 1 + \xi^2] r \, dr - \int_\Omega \alpha[\eta^2 - \mu] r \, dr,$$

where the constraints in (5) are adjoined to the functional π of eqn (10) by means of the Lagrangian multipliers Λ, $\lambda(r)$, $\beta(r)$, $\gamma(r)$ and $\alpha(r)$, and where the real slack-variables $\sigma(r)$, $\tau(r)$, $\xi(r)$ and $\eta(r)$ are introduced for converting the inequality constraints on $h_s(r)$ and $\mu(r)$ to equality constraints.

The necessary condition for stationarity of π^* with respect to the design variable $\mu(r)$ is now found to be

$$(D_{max} - D_s)[(1-\nu^2)\kappa_{\theta\theta}^2 + 2(1-\nu)\kappa_{r\theta}^2] + D_r^2\left(\frac{1}{D_s} - \frac{1}{D_{max}}\right)(\kappa_{rr} + \nu\kappa_{\theta\theta})^2 \tag{12}$$

$$= \Lambda(h_{max} - h_s) + \gamma(r) - \alpha(r),$$

and the stationarity condition with respect to the design variable $h_s(r)$ becomes

$$3h_s^2(1-\mu)[(1-\nu^2)\kappa_{\theta\theta}^2 + 2(1-\nu)\kappa_{r\theta}^2] + \frac{3(1-\mu)}{h_s^4} D_r^2(\kappa_{rr} + \nu\kappa_{\theta\theta})^2$$

$$= \Lambda(1-\mu) + \lambda(r) - \beta(r). \tag{13}$$

Conditions of stationarity of π^* with respect to the Lagrangian multipliers Λ, λ, β, γ and α reestablish the plate volume constraint and the maximum and minimum constraints on $h_s(r)$ and $\mu(r)$ in (5), and stationarity with respect to the slack variables σ, τ, ξ and η leads to switching conditions which, when combined with the constraints on h_s and μ, may be expressed together with appropriate Kuhn–Tucker conditions as follows,

$$\gamma(r) = 0, \ \alpha(r) \geq 0 \text{ if } \mu(r) \quad = 0$$

$$\gamma(r) = 0, \ \alpha(r) \qquad\qquad = 0 \text{ if } 0 \qquad < \mu(r) < 1 \qquad (14)$$

$$\gamma(r) \geq 0, \ \alpha(r) \qquad\qquad = 0 \text{ if } \mu(r) \qquad = 0$$

and

$$\lambda(r) = 0, \ \beta(r) \geq 0 \text{ if } h_s \quad = h_{min}$$

$$\lambda(r) = 0, \ \beta(r) = 0 \text{ if } h_{min} < h_s(r) < h_{max} \qquad (15)$$

$$\lambda(r) \geq 0, \ \beta(r) = 0 \text{ if } h_s \quad = h_{max}.$$

Equations (12) and (13) above constitute the two optimality conditions that are associated with the regularized formulation of the problem. The left-hand sides of these equations identify the gradients of the specific strain energy with respect to $\mu(r)$ and $h_s(r)$, respectively, and taking eqns (14) and (15) into account, eqns (12) and (13) show that in sub-regions where one of the design variables $\mu(r)$ and $h_s(r)$ is unconstrained, the gradient of the specific strain energy with respect to the particular design variable, should be constant.

By means of eqns (12)–(15), we are now able to derive specific conditions for the occurrence of sub-regions with integral stiffeners and of purely solid sub-regions of intermediate thickness in the optimal design.

3.1 Necessary condition for sub-regions with integral stiffeners
An integrally stiffened sub-region is characterized by

$$0 < \mu(r) < 1, \ h_{min} \leq h_s(r) < h_{max}. \qquad (16)$$

In view of inequalities (16) and the second of eqns. (14), eqn (12) reduces to

$$\frac{D_{max} - D_s}{h_{max} - h_s} [(1 - \nu^2)\kappa_{\theta\theta}^2 + 2(1 - \nu)\kappa_{r\theta}^2] + \frac{D_r^2}{h_{max} - h_s} \left(\frac{1}{D_s} - \frac{1}{D_{max}}\right)(\kappa_{rr} + \nu\kappa_{\theta\theta})^2 = \Lambda. \qquad (17)$$

Taking inequalities (16) and the first two of eqns (15) into account, we may express eqn (13) as

$$3h_s^2[(1 - \nu^2)\kappa_{\theta\theta}^2 + 2(1 - \nu)\kappa_{r\theta}^2] + \frac{3}{h_s^4} D_r^2(\kappa_{rr} + \nu\kappa_{\theta\theta})^2 \leq \Lambda. \qquad (18)$$

Eliminating Λ between eqn (17) and inequality (18), and expressing D_r, D_s and D_{max} in terms of μ, h_s and h_{max} by means of eqns (9) and the first of eqns (8), we after dividing through by $h_{max} - h_s$ obtain the necessary condition

$$(2h_s + h_{max})[(1 - \nu^2)\kappa_{\theta\theta}^2 + 2(1 - \nu)\kappa_{r\theta}^2] \geq \frac{h_{max}^3 h_s^2}{[\mu h_s^3 + (1 - \mu)h_{max}^3]^2} (h_s^2 + 2h_s h_{max} + 3h_{max}^2)(\kappa_{rr} + \nu\kappa_{\theta\theta})^2 \qquad (19)$$

for an integrally stiffened sub-region in the optimal design of a rotationally symmetric plate.

3.2 Necessary condition for purely solid sub-regions of intermediate thickness
A purely solid sub-region of intermediate thickness is associated with

$$\mu(r) = 0, \ h_{min} < h_s(r) < h_{max}. \qquad (20)$$

By eqns (20) and the first of eqns (14), and noting that $D_r = D_s$ for $\mu = 0$, the optimality condition (12) may thus be written as

$$\frac{D_{\max} - D_s}{h_{\max} - h_s}[(1 - \nu^2)\kappa_{\theta\theta}^2 + 2(1 - \nu)\kappa_{r\theta}^2] + \frac{D_s(D_{\max} - D_s)}{D_{\max}(h_{\max} - h_s)}(\kappa_{rr} + \nu\kappa_{\theta\theta})^2 \le \Lambda, \qquad (21)$$

while the optimality condition (13) reduces to

$$3h_s^2[(1 - \nu^2)\kappa_{\theta\theta}^2 + 2(1 - \nu)\kappa_{r\theta}^2] + 3h_s^2(\kappa_{rr} + \nu\kappa_{\theta\theta})^2 = \Lambda \qquad (22)$$

since h_s is unconstrained and $\mu \ne 0$.

Combining eqns (21) and (22), using eqns (9), and dividing through by $h_{\max} - h_s$, we obtain the inequality

$$(2h_s + h_{\max})[(1 - \nu^2)\kappa_{\theta\theta}^2 + 2(1 - \nu)\kappa_{r\theta}^2] \le$$

$$+ \frac{h_s^2}{h_{\max}^3}(h_s^2 + 2h_s h_{\max} + 3h_{\max}^2)(\kappa_{rr} + \nu\kappa_{\theta\theta})^2, \qquad (23)$$

which constitutes a *necessary condition for a purely solid sub-region of intermediate thickness in the optimal design of a rotationally symmetric plate*.

Unfortunately, it does not seem possible to derive specific conditions for purely solid sub-regions of minimum thickness $h_{\min}$ or maximum thickness $h_{\max}$ on the present basis.

3.3 Behaviour of the optimal design in the vicinity of plate edges

At a simply supported or free plate edge, we have $m_{rr} = 0$, which is equivalent to $\kappa_{rr} + \nu\kappa_{\theta\theta} = 0$, since singular behaviour is excluded via the condition that $h_s(\ge h_{\min}) > 0$. With $\kappa_{rr} + \nu\kappa_{\theta\theta} = 0$ and $(1 - \nu^2)\kappa_{\theta\theta}^2 + 2(1 - \nu)k_{r\theta}^2 > 0$ in general for a simply supported or free edge, and $2h_s + h_{\max} > 0$, it is readily seen that the condition 23) is not satisfied.

Hence, *a purely solid sub-region of intermediate thickness will never appear at a simply supported or free edge of an optimally designed rotationally symmetric plate*. The optimal plate will either be integrally stiffened (note that condition (19) is satisfied) or solid with minimum or maximum thickness in the vicinity of a simply supported or free edge.

At a clamped edge $r = r^*$ of an axisymmetric plate, we have $w(r^*) = w'(r^*) = 0$, and hence $\kappa_\theta(r^*) = \kappa_{r\theta}(r^*) = 0$. In view of the latter conditions, the fact that $h_s^2 + 2h_s h_{\max} + 3h_{\max}^2 > 0$ and that $(\kappa_{rr}(r^*) + \nu\kappa_{\theta\theta}(r^*))^2 > 0$ in general for a clamped edge, we see that condition (19) fails to be satisfied.

Thus, *a sub-region with integral circumferential stiffeners will not be found at a clamped edge of an optimally designed rotationally symmetric plate*. In the vicinity of such an edge, the plate will be purely solid, and its edge thickness will belong to the interval $h_{\min} \le h_s \le h_{\max}$.

The above results constitute a generalization of some very recent results obtained in [11] for a slightly different problem by means of the Kelley condition from optimal control theory.

3.4 Discussion

The necessary condition (23) for optimality of a solid sub-region of intermediate thickness may be expressed in an alternative way. Firstly, define a thickness parameter α by

$$\alpha = \frac{h_s}{h_{\max}}, \qquad (24)$$

write inequality (23) as

$$\frac{(\kappa_{rr} + \nu\kappa_{\theta\theta})^2}{\kappa_{rr}^2 + 2\nu\kappa_{rr}\kappa_{\theta\theta} + \kappa_{\theta\theta}^2 + 2(1 - \nu)\kappa_{r\theta}^2} \ge \frac{1 + 2\alpha}{(1 + \alpha + \alpha^2)^2}, \qquad (25)$$

and note then that since $\mu(r) = 0$ in a solid sub-region of intermediate thickness h_s, the moment-curvature relationships (7a or b) reduce to those that are valid for solid, isotropic

plates, i.e.

$$m_{rr} = h_s{}^3(\kappa_{rr} + \nu\kappa_{\theta\theta}), \quad m_{\theta\theta} = h_s{}^3(\kappa_{\theta\theta} + \nu\kappa_{rr}), \quad m_{r\theta} = h_s{}^3(1 - \nu)\kappa_{r\theta}. \tag{26}$$

Then, using eqns (26) to eliminate the curvatures in (25), we obtain

$$\frac{m_{rr}^2}{m_{rr}^2 - 2\nu m_{rr}m_{\theta\theta} + m_{\theta\theta}^2 + 2(1 + \nu)m_{r\theta}^2} \geq \frac{1 + 2\alpha}{(1 - \nu^2)(1 + \alpha + \alpha^2)^2}, \tag{27}$$

which constitutes an alternative to inequality (23). The necessary condition (27), which the moments and the plate thickness $h_s = \alpha h_{max}$ must satisfy for optimality of an intermediate, purely solid sub-region, is very similar to one derived in Ref. [12], eqn (II64). The only difference is that the moments of the two conditions refer to different structures.

Let us now consider the special case where our plate is subjected to axisymmetric load ($n = 0$). Then, the θ-independent factorial $m_{r\theta}$ of the twisting moment vanishes everywhere, and introducing the moment parameter λ by

$$\lambda = \frac{m_{\theta\theta}}{m_{rr}}, \tag{28}$$

inequality (27) may be cast in the form

$$\frac{1}{1 - 2\nu\lambda + \lambda^2} \geq \frac{1 + 2\alpha}{(1 - \nu^2)(1 + \alpha + \alpha^2)^2}. \tag{29}$$

This inequality partitions the $\lambda - \alpha$ plane into two separate regions, see Fig. 2 (which presumes $\nu = 0.25$). In Fig. 2, combinations of λ and α for which inequality (29) is not satisfied, fall in the hatched region. Consequently, combinations of λ and α calculated on the basis of the thickness and moments at points belonging to an intermediate, purely solid sub-region in an optimal design must be within the unhatched region. At a clamped plate edge, for example, we have $\lambda = m_{\theta\theta}/m_{rr} = \nu$, and the figure illustrates that for values of α belonging to the interval $h_{min}/h_{max} < \alpha < 1$, all combinations of λ and α will lie within the unhatched region, which implies that a purely solid sub-region of intermediate thickness is optimal in the neighbourhood of the clamped edge. If $\alpha = h_{min}/h_{max}$ or $\alpha = 1$ at the clamped edge, the optimal plate will be
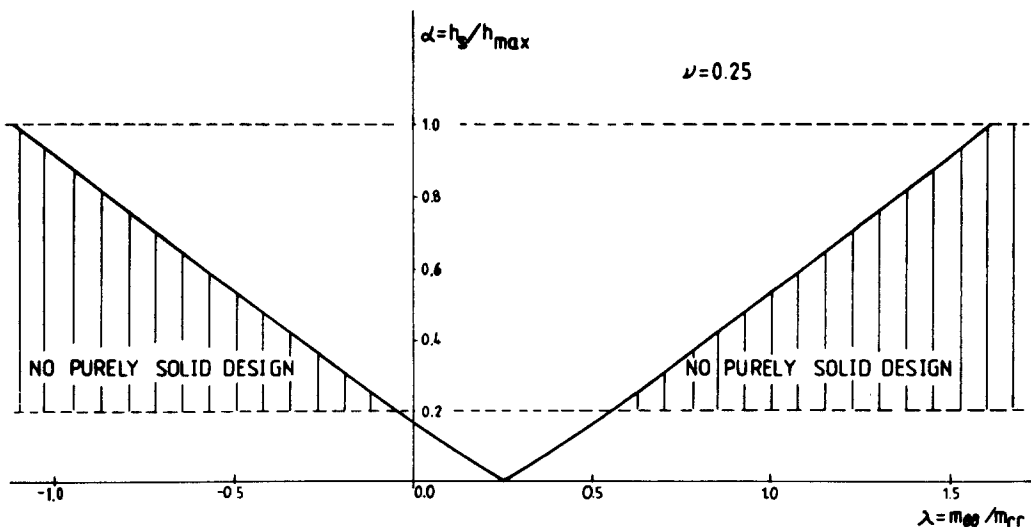

Fig. 2. $\lambda - \alpha$ diagram for axisymmetric plates ($\nu = 0.25$) optimized for minimum static compliance under axisymmetric load or maximum fundamental natural frequency of transverse vibrations ($n = 0$). If the combination (λ, α) for a given plate point falls in the hatched area of the diagram, the optimal design cannot be purely solid at the point considered.

solid and of thickness $h_s = h_{min}$ or $h_s = h_{max}$, respectively, at the edge. At a simply supported or free edge, $\lambda \to \pm\infty$, and any combination of λ and α will then lie in the hatched region of Fig. 2, which means that either an integrally stiffened sub-region or a purely solid sub-region of thickness $h_s = h_{min}$ or $h_s = h_{max}$, respectively, will be optimal near the simply supported or free edge.

Figure 2 may be compared with Fig. 7 of Ref. [10]. In spite of their strong resemblence, these two figures are different. The latter figure is not restricted to axisymmetric plates, as the local direction of the stiffeners may be chosen optimally. Figure 2 of the present paper, however, is obtained under the assumption that all the stiffeners follow the circumferential direction of the plate. This clearly limits the efficiency of the stiffeners, and it is therefore not surprising that the unhatched region with optimality of purely solid sub-regions is much larger in Fig. 2 of the present paper than in Fig. 7 of Ref. [10].

4. DESIGN FOR MAXIMUM TRANSVERSE VIBRATION FREQUENCY

Consider now the·problem of determining the optimal thickness distribution for a solid, elastic, axisymmetric, annular (or full) plate, which, for given total volume, plate radii, boundary conditions and elastic moduli, maximizes the smallest natural frequency ω_n corresponding to a vibration mode

$$W(r, \theta) = w(r) \cos n\theta \qquad (30)$$

that has a prescribed number n $(n \geq 0)$ or nodal diameters. Again, the plate optimization problem is geometrically constrained, that is, minimum and maximum constraint values, h_{min} and h_{max}, respectively, are specified for the plate thickness function.

To extend the design space relative to earlier results, we use the new plate model shown in Fig. 1 and apply both the concentration $\mu(r)$ of integral stiffeners and the thickness h_s of the solid part of the plate as design variables. Hence, the following regularized formulation of the problem is considered:

With $h_s(r)$ and $\mu(r)$ as design variables, maximize

$$\omega_n^2 = \frac{\int_\Omega \{D_{r\theta}(r)[(1-\nu^2)\kappa_{\theta\theta}^2(r) + 2(1-\nu)\kappa_{r\theta}^2(r)] + D_r(r)(\kappa_{rr}(r) + \nu\kappa_{\theta\theta}(r))^2\}r\,\mathrm{d}r}{\int_\Omega [h_s(r) + \mu(r)(h_{max} - h_s(r))]w^2(r)r\,\mathrm{d}r}$$

subject to the constraints

$$\int_\Omega [h_s(r) + \mu(r)(h_{max} - h_s(r))]r\,\mathrm{d}r = 1, \quad h_{min} \leq h_s(r) \leq h_{max}, \quad 0 \leq \mu(r) \leq 1, \qquad (31)$$

where

$$r \in \Omega\{r|R_i \leq r \leq 1\}.$$

The problem is in non-dimensional form, and the first of eqns (31) expresses the Rayleigh quotient for the new plate model in transverse vibration of the type (30), see [11]. The bending rigidity moduli $D_{r\theta}$ and D_r for the new plate model are defined in eqn (8), and the curvatures κ_{rr}, $\kappa_{\theta\theta}$ and $\kappa_{r\theta}$ are given in terms of the θ-independent factorial $w(r)$ of the deflection and the number n of nodal diameters by eqns (6). The second of eqns (31) expresses in dimensionless form the fact that the total plate volume is given.

To derive the necessary conditions for optimality, we apply calculus of variations and construct a functional F by adjoining to the expression for ω_n^2 in the first of eqns (31), the subsequent constraint conditions in eqns (31) by means of the Lagrangian multipliers Λ, $\lambda(r)$,

$\beta(r)$, $\gamma(r)$ and $\alpha(r)$, i.e.

$$F = \frac{\int_{\Omega} \{D_{r\theta}[(1-\nu^2)\kappa_{\theta\theta}^2 + 2(1-\nu)\kappa_{r\theta}^2] + D_r(\kappa_{rr} + \nu\kappa_{\theta\theta})^2\} r \, dr}{\int_{\Omega} [h_s + \mu(h_{max} - h_s)]w^2 \, dr}$$

$$-\Lambda\left\{\left[\int_{\Omega} [h_s + \mu(h_{max} - h_s)]\right] r \, dr - 1\right\}$$

$$-\int_{\Omega} \lambda[h_s - h_{max} + \sigma^2] r \, dr - \int_{\Omega} \beta[h_{min} - h_s + \tau^2] r \, dr \tag{32}$$

$$-\int_{\Omega} \gamma[\mu - 1 + \xi^2] r \, dr - \int_{\Omega} \alpha[\eta^2 - \mu] r \, dr.$$

The Euler–Lagrange equation expressing stationarity of F with respect to the design variable $\mu(r)$ is now

$$(D_{max} - D_s)[(1-\nu^2)\kappa_{\theta\theta}^2 + 2(1-\nu)\kappa_{r\theta}^2] + D_r^2\left(\frac{1}{D_s} - \frac{1}{D_{max}}\right)(\kappa_{rr} + \nu\kappa_{\theta\theta})^2$$

$$-\omega^2(h_{max} - h_s)w^2 - \Lambda(h_{max} - h_s) - \gamma(r) + \alpha(r) = 0, \tag{33}$$

and stationarity with respect to the design variable $h_s(r)$ leads to

$$3h_s^2(1-\mu)[(1-\nu^2)\kappa_{\theta\theta}^2 + 2(1-\nu)\kappa_{r\theta}^2] + \frac{3(1-\mu)}{h_s^4} D_r^2(\kappa_{rr} + \nu\kappa_{\theta\theta})^2$$

$$-\omega^2(1-\mu)w^2 - \Lambda(1-\mu) - \lambda(r) + \beta(r) = 0. \tag{34}$$

In the derivation of eqns (33) and (34), it is assumed that the vibration mode w is normalized according to

$$\int_{\Omega} [h_s + \mu(h_{max} - h_s)]w^2 r \, dr = 1. \tag{35}$$

Equations (33) and (34) constitute the so-called optimality conditions for the plate frequency optimization problem, and were first derived in Ref. [11] by means of optimal control theory. These optimality conditions are seen to be the same as the corresponding conditions (12) and (13) for the static compliance minimization problem, except that they both contain an additional non-linear term pertaining to the dynamic nature of the problem.

Finally, stationarity of F with respect to variation of the Lagrangian multipliers Λ, $\lambda(r)$, $\beta(r)$, $\gamma(r)$ and $\alpha(r)$ recovers the constraints in eqns (31), and stationarity with respect to the slack-variables $\sigma(r)$, $\tau(r)$, $\xi(r)$ and $\eta(r)$, together with appropriate Kuhn–Tucker conditions, gives us the switching conditions in the same form as eqns (14) and (15).

Let us now consider the question concerning conditions for integrally stiffened sub-regions and purely solid sub-regions of intermediate thickness, respectively, for the plate frequency optimization problem. For a sub-region with integral stiffeners, we have $0 < \mu(r) < 1$, $h_{min} \le h_s(r) < h_{max}$, and hence $\lambda(r) = \gamma(r) = \alpha(r) = 0$, $\beta(r) \ge 0$, see eqns (14) and (15), which implies that optimality conditions (33) and (34) reduce to

$$\frac{D_{max} - D_s}{h_{max} - h_s}[(1-\nu^2)\kappa_{\theta\theta}^2 + 2(1-\nu)\kappa_{r\theta}^2] + \frac{D_r^2}{h_{max} - h_s}\left(\frac{1}{D_s} - \frac{1}{D_{max}}\right)(\kappa_{rr} + \nu\kappa_{\theta\theta})^2 - \omega^2 w^2 = \Lambda \tag{36}$$

and

$$3h_s^2[(1-\nu^2)\kappa_{\theta\theta}^2 + 2(1-\nu)\kappa_{r\theta}^2] + \frac{3}{h_s^4} D_r^2(\kappa_{rr} + \nu\kappa_{\theta\theta})^2 - \omega^2 w^2 \le \Lambda, \tag{37}$$

respectively, which may be compared with eqns (17) and (18). Eliminating Λ between eqns (36) and (37), as in the linking of eqns (17) and (18) earlier, the additional term $-\omega^2 w^2$ drops out, and we end up with the result that *the necessary condition* (19) *also holds good for integrally stiffened sub-regions* (with $0 < \mu < 1$, $h_{min} \leq h_s < h_{max}$) *in optimal plates of maximum vibration frequency*. Similarly, we easily find that *the necessary condition* (23) *also governs optimality of a purely solid sub-region of intermediate thickness* ($\mu = 0$, $h_{min} < h_s < h_{max}$) *in optimal plates of maximum vibration frequency*.

It follows from the results just cited that all the results and conclusions of Sections 3.3 and 3.4 hold good for the plate vibration frequency optimization problem as well. Hence, as is anticipated in Refs. [9, 10], the idea of investigating inherent features of plate optimization by considering the design criterion of minimum static compliance, which is simpler than other design criteria, is fully justified.

5. NUMERICAL RESULTS AND DISCUSSION

This section presents numerical solutions to the regularized formulations for minimization of plate compliance and maximization of plate vibration frequency considered in the foregoing. The solution procedure is outlined in the Appendix. The solutions are obtained by sub-dividing the plate into 100 elements in examples of compliance minimization, and into 150 elements in examples of frequency maximization. In the following, the compliance π or frequency ω_n of each optimal plate will be stated in proportion to the corresponding compliance π_u or frequency ω_n^u of a purely solid, uniform reference plate of thickness h_u that has the same total volume, plate radii and boundary conditions, and is made of the same material as the optimized plate. Poisson's ratio of the plate material is taken to be $\nu = 0.25$. In the examples of compliance minimization, the uniform reference plate is, of course, subjected to the same static loading as the optimal plate. Although we are able to cope with arbitrary static loading in the form of eqn (1), we take $f(r) = \text{const.}$ in the examples of compliance minimization.

Figures 3–5 show radial sections through optimal, axisymmetric plates. In each figure, the unhatched area indicates the solid part of the plate, whose thickness is $h_s(r)$, and hatched areas indicate that integral stiffeners of total height $(h_{max} - h_s)$ are placed symmetrically with respect to the plate mid-plane. The sum of the extents of the upper and lower hatched areas in the normal direction at a specific value of the radial coordinate r, represents $\mu(r) \cdot (h_{max} - h_s(r))$ of the design. This function is plotted to the same scale as $h_s(r)$ in the figures, and illustrates the material consumption of the integral stiffeners by an equivalent thickness of purely solid material. The solid curve shown above each plate is the θ-independent factorial $w(r)$ of the deflection function. Different scales are used for these curves in the figures.

Figures 3(a)–(c) show minimum compliance designs of axisymmetric, annular plates with clamped inner and outer edges. The designs all have $h_u/h_{min} = 1.6579$, $h_{max}/h_{min} = 5$ and $R_i = 0.2$, and they serve to illustrate the influence on the optimal design of the circumferential wave number n of the external loading, eqn (1). The optimal design in Fig. 3(a) corresponds to $n = 0$, i.e. axisymmetric load, and the designs in Fig. 3(b) and (c) correspond to $n = 2$ and $n = 4$, respectively, i.e. loads of the form $p(r, \theta) = \text{const} \cdot \cos 2\theta$ and $p(r, \theta) = \text{const} \cdot \cos 4\theta$. The compliances of the optimal designs are found to be $\pi/\pi_u = 0.463$, 0.491 and 0.357, for $n = 0, 2$ and 4, respectively.

The results in Fig. 3 clearly show that the significance of integral, circumferential stiffeners increases with increasing n. In the case of axisymmetric load, the optimal design, Fig. 3(a), is almost entirely a purely solid plate, and only an examination of the numerical data reveals that a small sub-region with very low stiffener concentration is present. However, for $n = 4$ (Fig. 3c), most of the material volume, which is available for design in view of the minimum thickness constraint, is used for formation of stiffeners, and only small, solid sub-regions of intermediate thickness are found near the clamped edges of the plate.

Figures 4(a)–(c) show three full circular plates optimized for maximum fundamental natural frequency ($n = 0$). The plates all have clamped edges and $h_u/h_{min} = 1.5915$, and the only difference in their design conditions is that different values of the ratio h_{max}/h_{min} are specified, namely $h_{max}/h_{min} = 5$, 10 and 15 in Figs. 4(a), (b) and (c), respectively.

By mutual comparison of Figs. 4(a)–(c), we see that an increasing part of the plate volume is used for the formation of integral stiffeners as the maximum thickness constraint value h_{max} is
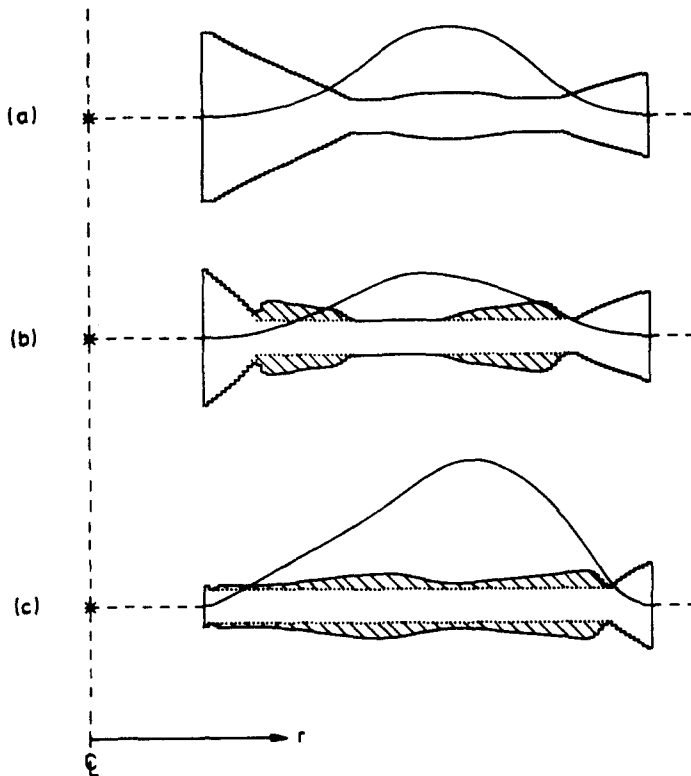
Fig. 3. Axisymmetric annular plates of minimum compliance subject to different loads $p = \text{const} \cdot \cos n\theta$. The designs correspond to $h_u/h_{min} = 1.6579$, $h_{max}/h_{min} = 5$, $R_i = 0.2$ and $\nu = 0.25$. Plate edges are clamped. (a) $n = 0$, $\pi/\pi_u = 0.463$; (b) $n = 2$, $\pi/\pi_u = 0.491$; (c) $n = 4$, $\pi/\pi_u = 0.357$.
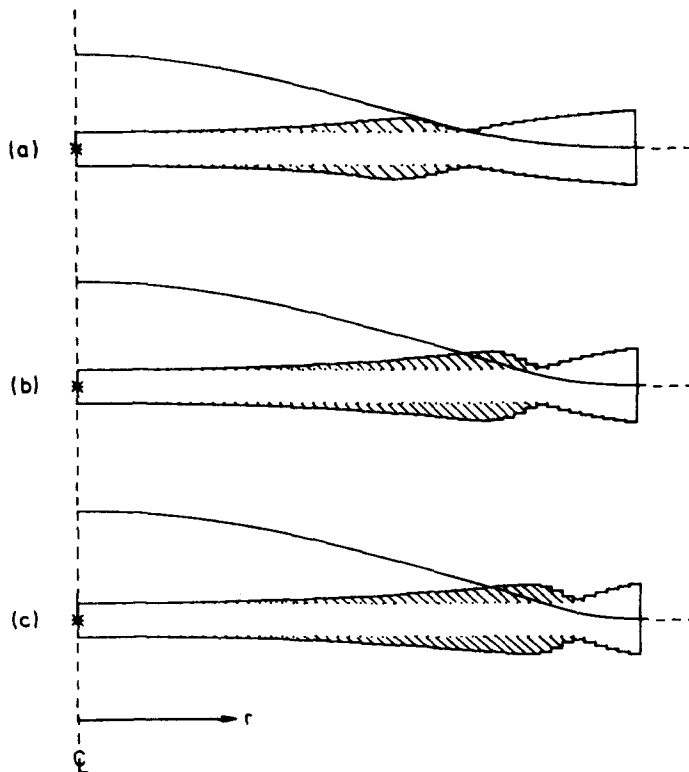

Fig. 4. Axisymmetric, clamped plates of different h_{max}/h_{min} ratios optimized for maximum fundamental natural transverse vibration frequency, ω_0. (a) $h_{max}/h_{min} = 5$, $\omega_0/\omega_0^u = 1.43$; (b) $h_{max}/h_{min} = 10$, $\omega_0/\omega_0^u = 2.06$; (c) $h_{max}/h_{min} = 15$, $\omega_0/\omega_0^u = 2.72$. The plates have equal volume, given by $h_u/h_{min} = 1.5915$, and Poisson's ratio is $\nu = 0.25$ for the plate material.

increased. Coincidently, we find that the value of the optimal fundamental frequency ω_0 increases with h_{max}, viz. $\omega_0/\omega_0^u = 1.43$, 2.02 and 2.72 for $h_{max}/h_{min} = 5$, 10 and 15, respectively. This is in perfect agreement with the fact that the fundamental natural frequency of a plate can be increased indefinitely by geometrically unconstrained optimization. Note also the circum-ferential stiffeners do not arise near the clamped plate edges of Figs. 3 and 4, but that purely solid sub-regions of intermediate thickness are found in their vicinities.

Figures 5(a)–(e) show minimum compliance designs (Figs. 5a, b) and maximum frequency designs (Figs. 5c–e) of annular plates of different boundary conditions (see the figure caption). These numerical solutions are obtained for $h_{max}/h_{min} = 5$, $h_u/h_{min} = 1.6579$ and $n = 4$, and serve to illustrate the theoretical predictions of Sections 3.3 and 5 for the behaviour of the optimal design near plate edges.

In agreement with the theoretical predictions, and independently of the design criteria, we see that the clamped edges only have purely solid sub-regions in their vicinities, and that the free and simply supported edges have either stiffened sub-regions or purely solid ones of $h_s = h_{min}$ or $h_s = h_{max}$ (but never $h_{min} < h_s < h_{max}$) in their neighbourhood.

Let us now compare a series of minimum compliance results obtained by the present formulation for optimal design to corresponding results obtained by earlier formulations. All the results pertain to $n = 4$ for annular plates with $R_i = 0.2$, $h_{max}/h_{min} = 5$ and $h_u/h_{min} = 1.6579$, and are given in Table 1. The first column in Table 1 lists three different combinations of boundary conditions at the inner and outer plate edge. Each of the next three columns list, for each set of plate boundary conditions, the ratio π/π_u, where the plate compliance π is minimized in applying a particular formulation for optimal design. Within any given row of the table, the design conditions and the value π_u for a uniform, solid reference plate of the same boundary conditions are, of course, the same. Now, in the second column from the left, minimum values of π are determined via the traditional formulation ($\mu \equiv 0$), and the results are quoted from Ref. [9]. The third column presents minimum values of π obtained by means of the integrally stiffened plate formulation where $h_s(r) \equiv h_{min}$ and only $\mu(r)$ is treated as design variable. These results are taken from Ref. [10]. Finally, minimum compliances π determined on the basis of the regularized formulation of the present paper, where both $\mu(r)$ and $h_s(r)$ are design variables, are listed in the fourth column of Table 1.

On the basis of the results in Table 1, we are able to conclude that the regularized optimal plate design formulation of the present paper is superior to the earlier formulations. Since our new formulation implies an expansion of the design space and contains the design spaces of each of the earlier formulations as sub-spaces, it must, of course, for any given problem, be expected to offer a solution that is at least as good as the best solution offered by the earlier formulations. Table 1 demonstrates that results following from our new formulation will, in general, not be not just as good as, but significantly better than, results obtained from the earlier formulations.

The physical reason for the superiority of the present formulation over the formulation with $h_s \equiv h_{min}$ is clearly that the axisymmetric plate is offered the possibility of increasing locally its radial stiffness by forming sub-regions of intermediate thickness. If we expand our design space further by dropping the condition of axisymmetry, it is quite obvious that the plate would increase its radial stiffness by forming an additional field of stiffeners, and that solutions with even more optimal characteristics could be obtained.

Table 1. Comparison of minimum compliances π for axisymmetric annular plates determined via three different formulations for optimal design. The results correspond to $n = 4$, $R_i = 0.2$, $h_u/h_{min} = 1.6579$, $h_{max}/h_{min} = 5$ and $\nu = 0.25$

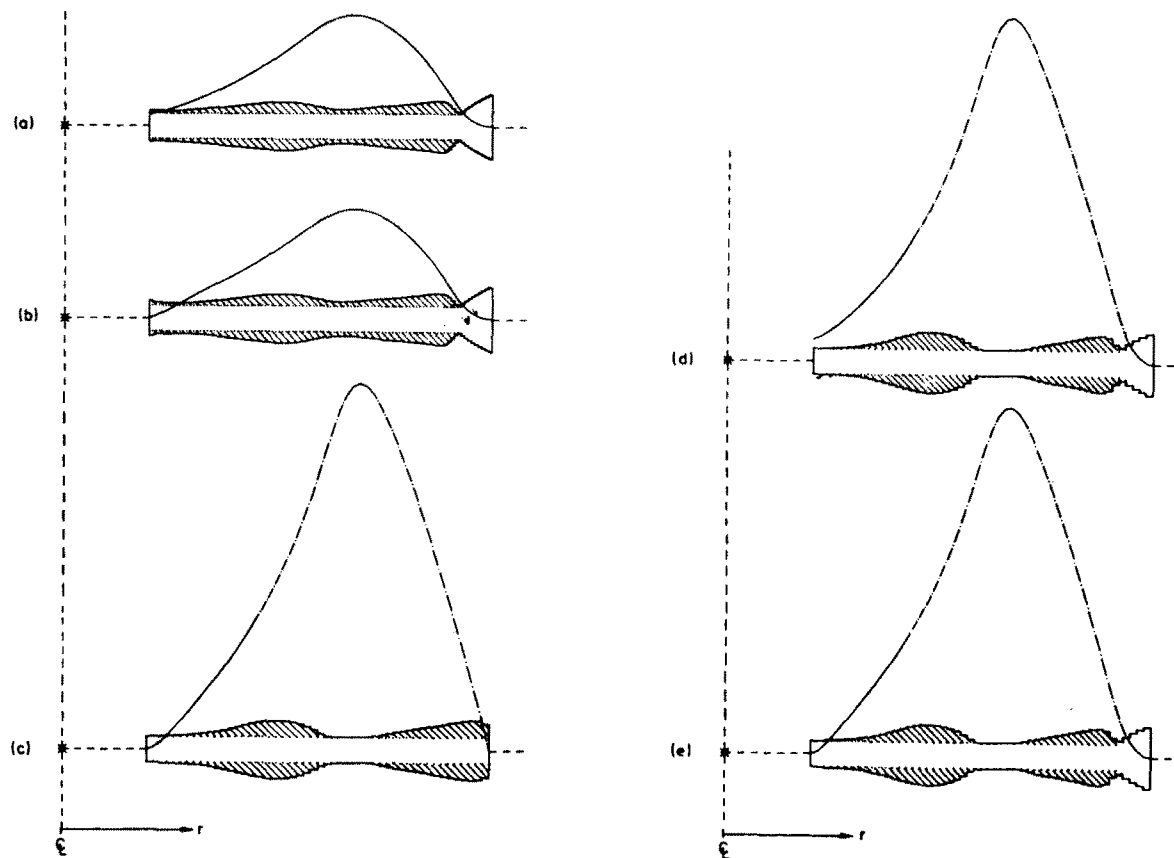|	π/π_u		
Boundary conditions at inner and outer plate edge	Traditional formulation ($\mu \equiv 0$), from [9]	Formulation with $h_s \equiv h_{min}$, from [10]	Regularized formulation of present paper
clamped-clamped	0.536	0.415	0.357
simply supp.-clamped	0.564	0.407	0.351
free-clamped	0.617	0.404	0.349

Fig. 5. Optimal, axisymmetric annular plates of different boundary conditions. The plates have h_a/h_{min} = 1.6579 and h_{max}/h_{min} = 5, and correspond to n = 4. Figs. 5(a), (b) illustrate minimum compliance designs. (a) Free inner edge and clamped outer edge, π/π_u = 0.349; (b) simply supported-clamped plate, π/π_u = 0.351; (see Fig. 3(c) for the corresponding clamped-clamped plate). Figs. 5(c)–(e) show maximum transverse vibration frequency designs. (c) clamped-simply supported plate, $\omega_a/\omega_4{}^u$ = 1.91; (d) free-clamped plate, $\omega_a/\omega_4{}^u$ = 1.77; (e) clamped-clamped plate, $\omega_a/\omega_4{}^u$ = 1.76.

The authors believe that the designs presented in this paper are global optimal designs within the type of plate topology considered here. However, these designs are obtained as solutions to a somewhat idealized mathematical formulation, and it is obvious that they must be regarded as limiting designs from the point of view of practical application.

In practice it is necessary to modify the design, which implies a less optimal value of the performance index. Let us therefore end this paper with an assessment of the sensitivity of the current type of optimal designs with respect to their most necessary type of modification, namely lumping the system of infinitely many, infinitely thin integral stiffeners into a finite number of stiffeners of finite width (to meet non-buckling requirements, e.g.). As an example, consider the optimal design of Fig. 3(c); sub-divide it into 3, 4, 5 and 6 sections, respectively;

Table 2. Compliances π of optimized and modified designs of a clamped-clamped annular plate with $n = 4$, $R_i = 0.2$, $h_s/h_{min} = 1.6579$, $h_{max}/h_{min} = 5$ and $\nu = 0.25$

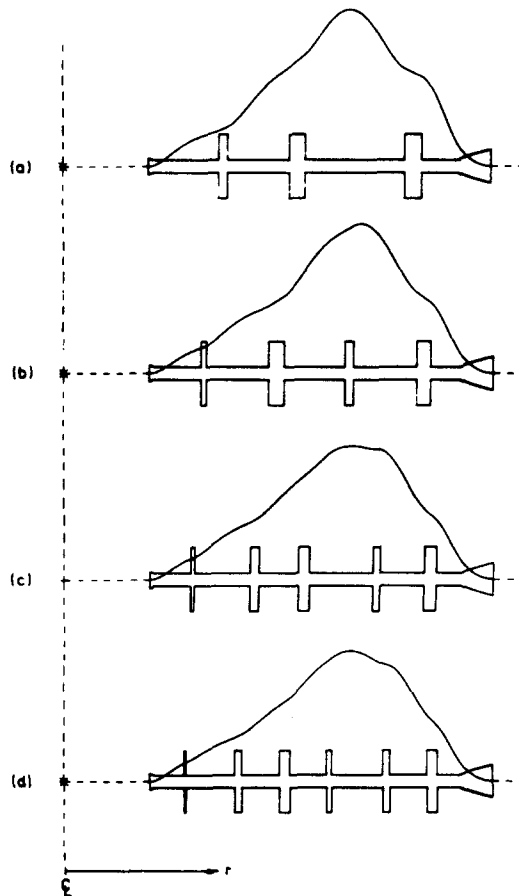|	π/π_u	
Traditional formulation ($\mu = 0$)	0.536	from [9]
Formulation with $h_s = h_{min}$	0.415	from [10]
Regularized formulation, optimal design	0.357	Fig. 3c
Modified opt. design, 3 lumped stiffeners	0.444	Fig. 6a
Modified opt. design, 4 lumped stiffeners	0.438	Fig. 6b
Modified opt. design, 5 lumped stiffeners	0.413	Fig. 6c
Modified opt. design, 6 lumped stiffeners	0.401	Fig. 6d

Fig. 6. Modified versions of the optimal design in Fig. 3(c), obtained by lumping the optimal distribution of integral stiffeners into a finite number of stiffeners of finite width. The compliances of the modified optimal designs are given in Table 2.

lump the infinitely thin stiffeners appropriately (which can be done in different ways), and obtain the series of modified designs shown in Figs. 6(a)–(d). The compliances of these modified designs are given in Table 2 together with minimum compliance values determined via the two earlier and the new formulation for optimal design. We see that even the design with only three lumped stiffeners has a lower compliance than the minimum value determined via the traditional formulation for optimal design. For the modified design with six lumped stiffeners, the compliance is already comparatively close to the compliance of the true optimal design. These results indicate clearly that optimal designs determined by means of new, regularized formulation are rather insensitive with respect to reasonable modification of the type considered.

REFERENCES

1. R. Reiss, Optimal compliance criterion for axisymmetric solid plates. *Int. J. Solids Structures* 12, 319–329 (1976).
2. K. A. Lurie and A. V. Cherkaev, Prager theorem application to optimal design of thin plates (in Russian). *MTT (Mechanics of Solids)* 13, 113–118 (1978).
3. N. Olhoff, Optimal design of vibrating rectangular plates. *Int. J. Solids Structures* 10, 93–109 (1974).
4. A. P. Seiranyan, A study of an extremum in the optimal problem of a vibrating circular plate (in Russian). *MTT (Mechanics of Solids)* 13, 113–118 (1978).
5. V. A. Grinev and A. P. Filippov, Optimum circular plates (in Russian). *MTT (Mechanics of Solids)* 12, 131–137 (1977).
6. N. M. Gura and A. P. Seiranyan, Optimum circular plate with constraints on the rigidity and frequency of natural oscillations (in Russian). *MTT (Mechanics of Solids)*, 12, 138–145 (1977).
7. J.-L. Armand, Numerical solutions in optimization of structural elements. *Paper Presented at 1st Int. Conf. on Computational Methods in Nonlinear Mechanics*, Austin, Texas, U.S.A. (Sept. 1974).
8. J.-L. Armand and B. Lodier, Optimal design of bending elements. *Int. J. Num. Meth. Engng* 13, 373–384 (1978).
9. K.-T. Cheng and N. Olhoff, An investigation concerning optimal design of solid elastic plates. *Int. J. Solids Structures* 17, 305–323 (1981).
10. K.-T. Cheng, On non-smoothness in optimal design of solid elastic plates. *Int. J. Solids Structures* 17, 795–810 (1981).
11. N. Olhoff, K. A. Lurie, A. V. Cherkaev and A. V. Fedorov, Sliding regimes and anisotropy in optimal design of vibrating axisymmetric plates. *Int. J. Solids Structures* 17, 931–948 (1981).
12. K.-T. Cheng, Optimal design of solid elastic plates. Ph.D. thesis, 97 pp., Dept. of Solid Mechanics, Technical University of Denmark, 1980.

APPENDIX

Here, we give an account of a numerical procedure of successive iterations, which is constructed for solving the regularized optimization problem with the two design variables $\mu(r)$ and $h_s(r)$. Since the solution methods for the minimum compliance and the maximum vibration frequency problems are very similar, we shall limit our description to the former type of problem.

In brief, the method is as follows: Starting with a given design, the finite element method is used for analysis of the structure such that all quantities pertaining to its deformation are determined. These results are then used to obtain an improved design by means of recurrence formulae derived from the two optimality conditions (12) and (13) of the problem. This procedure is repeated until the results become stationary.

The numerical procedure is based on a discretization of the problem, where the axisymmetric plate is sub-divided into a large number of concentric ring-elements of equal radial extent. Within each element, the design variables μ and h_s are assumed to attain constant values, and a complete third order polynomium for the deflection w is chosen as shape function. The values of w and w' at the intersection circles between the elements are used as nodal unknowns. The stiffness matrices corresponding to $D_{r\theta}$ and D_r are easily established by means of the energy expression (10), and it is then a straightforward matter to determine, for given design $\mu(r)$ and $h_s(r)$, the deflection w, slope w' and curvatures κ_{rr}, $\kappa_{\theta\theta}$ and $\kappa_{r\theta}$ as functions of r by means of the finite element method.

The development of recurrence formulae from optimality conditions (12) and (13) for improving a given design, will be outlined next. In order to be consistent with the assumption that the design variables are constant within the individual elements, it is necessary for the optimality conditions to be elementwise satisfied[12]. Multiply therefore through eqs (12) and (13) by $r/(h_{max} - h_s)$ and $r/(1 - \mu)$, respectively, and integrate over the interval $r_k \leq r \leq r_{k+1}$, of each element, $k = 1, 2, \ldots, K$, to obtain

$$\left\{\frac{D_{max} - D_s}{h_{max} - h_s}\right\}_k \frac{E_{1k}}{S_k} + \left\{\frac{D_r^2}{h_{max} - h_s}\left(\frac{1}{D_s} - \frac{1}{D_{max}}\right)\right\}_k \frac{E_{2k}}{S_k} = \Lambda + \gamma_k - \alpha_k \tag{A1}$$

and

$$\{3h_s^2\}_k \frac{E_{1k}}{S_k} + \left\{\frac{3D_r^2}{h_s^4}\right\}_k \frac{E_{2k}}{S_k} = \Lambda + \lambda_k - \beta_k, \tag{A2}$$

respectively. Here, the subscript k indicates reference to the kth element, and the quantities E_{1k}, E_{2k} and S_k are given by

$$E_{1k} = \int_{r_k}^{r_{k+1}} [(1 - \nu^2)\kappa_{\theta\theta}^2 + 2(1 - \nu)\kappa_{r\theta}^2]r\,dr$$

$$E_{2k} = \int_{r_k}^{r_{k+1}} (\kappa_{rr} + \nu\kappa_{\theta\theta})^2 r\,dr \tag{A3}$$

$$S_k = \frac{1}{2}(r_{k+1}^2 - r_k^2).$$

Recurrence formulae may now be constructed in different ways from eqns (A1) and (A2), but it is essential to recall that the l.h.s. of eqn (A1), i.e.

$$q_k = \left\{\frac{D_{max} - D_s}{h_{max} - h_s}\right\}_k \frac{E_{1k}}{S_k} + \left\{\frac{D_r^2}{h_{max} - h_s}\left(\frac{1}{D_s} - \frac{1}{D_{max}}\right)\right\}_k \frac{E_{2k}}{S_k}, \tag{A4}$$

identifies the gradient of the compliance π with respect to the design variable μ, and that the l.h.s. of eqn (A2),

$$g_k = \{3h_s^2\}_k \frac{E_{1k}}{S_k} + \left\{\frac{3D_r^2}{h_s^4}\right\}_k \frac{E_{2k}}{S_k}, \tag{A5}$$

is the gradient of π with respect to the design variable h_s. We therefore apply eqn (A1) for determining $\mu(r)$, and eqn (A2) for determining h_s. In sub-regions of unconstrained $\mu(r)$, eqns (A1) and (A3) may be combined to give $1 = g_k \Lambda^{-1}$, and similarly, we have $1 = g_k \Lambda^{-1}$ in sub-regions where h_s is unconstrained. Raising these equations to the power η and multiplying them by μ_k and h_{sk}, respectively, they take the form $\mu_k = \mu_k q_k^\eta \Lambda^{-\eta}$ and $h_{sk} = h_{sk} g_k^\eta \Lambda^{-\eta}$. On the basis of the latter equations, we now construct the following recurrence formulae, where the constraints on μ and h_s are taken into account,

$$\mu_k^{(j+1)} = \begin{cases} 0 & \text{if} \quad \mu_k^{(j)} q_k^\eta \Lambda^{-\eta} \le 0 \\ \mu_k^{(j)} q_k^\eta \Lambda^{-\eta} & \text{if} \quad 0 < \mu_k^{(j)} q_k^\eta \Lambda^{-\eta} < 1 \\ 1 & \text{if} \quad \mu_k^{(j)} q_k^\eta \Lambda^{-\eta} \ge 1 \end{cases} \tag{A6}$$

$$h_{sk}^{(j+1)} = \begin{cases} h_{min} & \text{if} \quad h_{sk}^{(j)} g_k^\eta \Lambda^{-\eta} \le h_{min} \\ h_{sk}^{(j)} g_k^\eta \Lambda^{-\eta} & \text{if} \quad h_{min} < h_{sk}^{(j)} g_k^\eta \Lambda^{-\eta} < h_{max} \\ h_{max} & \text{if} \quad h_{sk}^{(j)} g_k^\eta \Lambda^{-\eta} \ge h_{max}. \end{cases} \tag{A7}$$

In eqns (A6) and (A7), the superscripts (j) and $(j + 1)$ refer to the designs of the current and the subsequent iteration, respectively, and the gradients q_k and g_k are determined on the basis of the current design. The value of the power η in eqns (A6) and (A7) is chosen so that the iterative procedure converges.

The formulae (A6) and (A7) possess some disadvantages, however. For example, if the stiffener concentration $\mu(r)$ becomes equal to zero in a given region of the interval at some stage of the iteration procedure, $\mu(r)$ will in all subsequent iterations remain zero in that region. Moreover, it turns out that after the first few iterations, the iteration history gradually becomes oscillating. We therefore impose move-limits upon $\mu_k^{(j+1)}$ and $h_{sk}^{(j+1)}$, and use the following revised recurrence formulae,

$$\mu_k^{(j+1)} = \begin{cases} \max\{(1 - \xi)\mu_k^{(j)}, 0\} & \text{if} \quad \mu_k^{(j)} q_k^\eta \Lambda^{-\eta} \le \max\{(1 - \xi)\mu_k^{(j)}, 0\} \\ \mu_k^{(j)} q_k^\eta \Lambda^{-\eta} & \text{if} \quad \max\{(1 - \xi)\mu_k^{(j)}, 0\} < \mu_k^{(j)} q_k^\eta \Lambda^{-\eta} < \min\{(1 + \xi)\mu_k^{(j)}, 1\} \\ \min\{(1 + \xi)\mu_k^{(j)}, 1\} & \text{if} \quad \mu_k^{(j)} q_k^\eta \Lambda^{-\eta} \ge \min\{(1 + \xi)\mu_k^{(j)}, 1\} \end{cases} \tag{A8}$$

$$h_{sk}^{(j+1)} = \begin{cases} \max\{(1 - \xi)h_{sk}^{(j)}, h_{min}\} & \text{if} \quad h_{sk}^{(j)} g_k^\eta \Lambda^{-\eta} \le \max\{(1 - \xi)h_{sk}^{(j)}, h_{min}\} \\ h_{sk}^{(j)} g_k^\eta \Lambda^{-\eta} & \text{if} \quad \max\{(1 - \xi)h_{sk}^{(j)}, h_{min}\} < h_{sk}^{(j)} g_k^\eta \Lambda^{-\eta} < \min\{(1 + \xi)h_{sk}^{(j)}, h_{max}\} \\ \min\{(1 + \xi)h_{sk}^{(j)}, h_{max}\} & \text{if} \quad h_{sk}^{(j)} g_k^\eta \Lambda^{-\eta} \ge \min\{(1 + \xi)h_{sk}^{(j)}, h_{max}\}. \end{cases} \tag{A9}$$

The move-limit parameter ξ in the recurrence formulae (A8) and (A9) is assigned an initial value, but is automatically adjusted if the iteration history becomes non-monotonic. Once non-monotonicity occurs, we return to the design of the previous iteration and then apply the recurrence formulae with a decreased value of ξ.

The Lagrangian multiplier Λ in eqns (A8) and (A9) is determined from the condition that the total material volume of the plate is given, cf. the second of eqns (5). The discretized version of this condition is

$$\sum_{k=1}^{K} [h_{sk}^{(j+1)} + \mu_k^{(j+1)}(h_{max} - h_{sk}^{(j+1)})]S_k - 1 = 0. \tag{A10}$$

With $\mu_k^{(j+1)}$ and $h_{sk}^{(j+1)}$ expressed in terms of Λ by eqns (A8) and (A9), eqn (A10) may be conceived as an implicit, nonlinear algebraic equation for Λ, which can be written formally as

$$G(\Lambda) = 0. \tag{A11}$$

Evaluation of $G(\Lambda)$ for a given value of Λ can be directly performed by means of eqns (A8)–(A10), and we easily determine the Λ value that satisfies eqn (A11) by applying the bisection method. Note that this method in itself constitutes an iterative procedure, and that it involves substitution of the Λ trial value into the r.h.s. of eqns (A8) and (A9) at each iteration step.

The iteration scheme of the numerical solution procedure for our optimization problem may be summarized as follows:

BEGIN Set iteration counter $j = 1$. Take $\mu_k^{(1)}$ and $h_{sk}^{(1)}$, $k = 1, \ldots, K$, arbitrarily. Take $\pi^{(0)}$ to be large and assign suitable values of ξ and η.

I For the plate with integral stiffener concentration $\mu_k^{(j)}$ and solid plate thickness $h_{sk}^{(j)}$, compute bending rigidity components of eqns (8) and (9). Determine the plate deflection w by means of the finite element method. Calculate the curvatures by eqn (6). Determine the compliance $\pi^{(j)}$ by eqn (10) and the gradients $q_k^{(j)}$ and $g_k^{(j)}$ by eqns (A3)–(A5).

II If $\pi^{(j)} > \pi^{(j-1)}$, decrease the move-limit parameter ξ and set $j = j - 1$.

III Apply the bisection method to determine the value of Λ that satisfies eqn (A10), with $\mu_k^{(j+1)}$ and $h_{sk}^{(j+1)}$ given by eqns (A8) and (A9). By this process, which consists of an inner iteration loop, $\mu_k^{(j+1)}$ and $h_{sk}^{(j+1)}$ of the new plate design are also determined.

IV Go to I if μ_k and h_{sk}, and hence all other iterates, have not converged.

END